

Amorphous structures induced in monocrystalline silicon by mechanical loading

I. Zarudi^{a)}

School of Aerospace, Mechanical and Mechatronic Engineering, The University of Sydney, NSW 2006, Australia

J. Zou

Division of Materials and Centre for Microscopy and Microanalysis, The University of Queensland, QLD 4072, Australia

W. McBride

School of Physics, University of Melbourne, Victoria 3010, Australia

L. C. Zhang

School of Aerospace, Mechanical and Mechatronic Engineering, The University of Sydney, NSW 2006, Australia

(Received 10 November 2003; accepted 9 June 2004)

Different amorphous structures have been induced in monocrystalline silicon by high pressure in indentation and polishing. Through the use of high-resolution transmission electron microscopy and nanodiffraction, it was found that the structures of amorphous silicon formed at slow and fast loading/unloading rates are dissimilar and inherit the nearest-neighbor distance of the crystal in which they are formed. The results are in good agreement with recent theoretical predictions. © 2004 American Institute of Physics. [DOI: 10.1063/1.1779344]

Silicon is a fundamental material for electronic and photovoltaic technologies^{1–3} and as such its crystalline high-pressure phases have been studied extensively.^{1,4–18} More than ten crystalline polymorphs formed in different stress application schemes have been reported¹² and a variety of different techniques including high-resolution transmission electron microscopy (TEM),^{4,11} Raman spectroscopy,^{10,18} and x-ray diffraction¹⁶ were used to perform these investigations.

Amorphous silicon in semiconductor materials can be produced by deposition techniques, such as vacuum evaporation or sputtering,^{19–21} and usually contains defects, such as voids and impurities.²² It can also be produced by ion implantation where the amorphous structure depends upon the implantation conditions.²³ In addition, amorphous silicon may also be developed in high-pressure loading or by surface modification such as indentation.^{4,6,24,25} While the structure of amorphous silicon produced in this way has not yet been examined in detail, it is thought that several types of amorphous silicon exist due to the concept of polyamorphism.^{26,27} A recent theoretical investigation stated that amorphous structures could be developed in monocrystalline silicon.²⁸ In this letter, we demonstrate a detailed structural study on the amorphous structures developed in monocrystalline silicon by means of TEM and nanodiffraction.

Microindentation and polishing were used to generate amorphous silicon for this study. All experiments were performed on the (100) surfaces of monocrystalline silicon with indentation tests being conducted on an Ultra-Micro Indentation System-2000. The spherical indenter used had a nominal radius of 5 μm and the maximum indentation load applied was $P_{\text{max}}=30$ mN. Two loading/unloading rates, 0.6 mN/s and 3 mN/s, were used.

Polishing experiments were performed on PM5 Auto-Lap precision Surface Modification Machine (Logitech) in a closed environment with nitrogen to minimize the possible surface oxidation. The abrasives used were $\alpha\text{-Al}_2\text{O}_3$ and had an average radius of 25 nm. The nominal polishing pressure was 42 kPa and the table rotation speed was 52 rpm.

The $\langle 110 \rangle$ cross section TEM specimens were prepared using a tripod,²⁹ in which the material removed was continuously monitored and the sample position with respect to the tripod adjusted during mechanical thinning. Ion-beam thinning was then carried out to provide a sufficiently thin area for TEM investigations. TEM studies were carried out using a Philips CM12 transmission electron microscope operating at 120 kV and a JEOL JEM3000F field emission gun transmission electron microscope operating at 300 kV. The nanodiffraction patterns were recorded using a 1024×1024 pixel MegaScan charge coupled device (CCD) camera.

Figure 1, cross-sectional TEM images, showing amorphous structures attained by microindentation and polishing with three loading conditions: (1) Indentation ($P_{\text{max}}=30$ mN) with a slow loading/unloading rate (0.6 mN/s), (2) indentation ($P_{\text{max}}=30$ mN) with a high loading/unloading rate (3 mN/s), and (3) polishing with a pressure of 42 kPa. It is seen that condition (1) led to a complex transformation zone with a nearly hemispherical shape [see Fig. 1(a)]. The central part of the zone is crystalline⁴ and is composed of BC8 (a body-centered-cubic phase) and R8 (a rhombohedral phase) crystals. The amorphous silicon is located in the peripheral regions. The pockets of amorphous silicon are less than 100 nm in diameter and could only be studied by nanodiffraction. However, condition (2) created a homogeneous amorphous transformation zone without any crystalline particle [see Fig. 1(b)]. Similarly, condition (3) generated small amorphous pockets with a characteristic length of 20–30 nm [see Fig. 1(c)].

^{a)}Electronic mail: irena@aeromech.usyd.edu.au

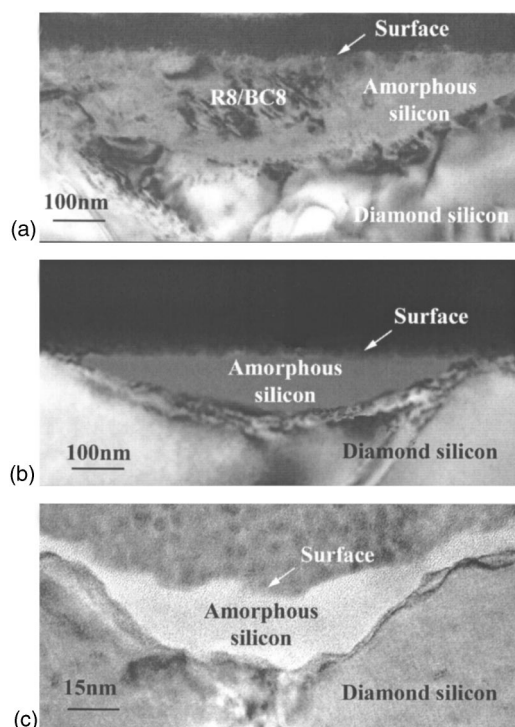


FIG. 1. Electron micrographs of amorphous structures in monocrystalline silicon after: (a) indentation with $P_{\max}=30$ mN, loading/unloading at 0.6 mN/s, (b) indentation with $P_{\max}=30$ mN, loading/unloading at 3 mN/s, and (c) polishing.

Figure 2 shows three nanodiffraction patterns of amorphous silicon that correspond to the three cases shown in Fig. 1. It is apparent that the typical continuous rings of amorphous materials are not obvious. The speckled ring structure takes place as a result of examining nanovolumes of material.³⁰ Figure 3 shows the radial profiles of Figs. 2(a)–2(c), obtained by azimuthal averaging.³¹ To perform the averaging, the location of the diffraction pattern's center was determined by fitting circles to intensity contours in the diffraction pattern using a least-squares method.³²

By comparing the three curves shown in Fig. 3, it is clear that the amorphous silicon structures formed in the three nanomodification processes are different. While disordered materials do not exhibit ordering over the large length scales that gives rise to the regular arrays of spots observed in crystalline diffraction patterns, there are still strong correlations in atomic positions that are less than 1 nm apart. This structure is observed as diffuse rings/peaks in the amorphous diffraction pattern.²⁸ As such, the differences in the diffuse ring structure observed in the three nanodiffraction patterns indicate that there are differences in the atomic structure of the amorphous silicon, over a 1 nm length scale, from which these diffraction patterns were taken.

The diffraction pattern from the amorphous silicon generated by condition (2) (curve 3 in Fig. 3) has a peak at $3.6\text{--}3.8\text{ nm}^{-1}$, corresponding to an atomic distance in the range of $2.5\text{--}2.8\text{ \AA}$. This suggests that the amorphous structure was formed from β -Sn (tetragonal structure with $a=4.68\text{ \AA}$ and $c=2.58\text{ \AA}$) silicon directly, having a six-coordinate ring with four distances of 2.43 \AA and two of 2.58 \AA .³³ The results are more understandable if the structural transformation events in indentation are recalled, in which the first phase transformation is to form the β -Sn phase during a loading process.⁴ In previous studies, the pos-

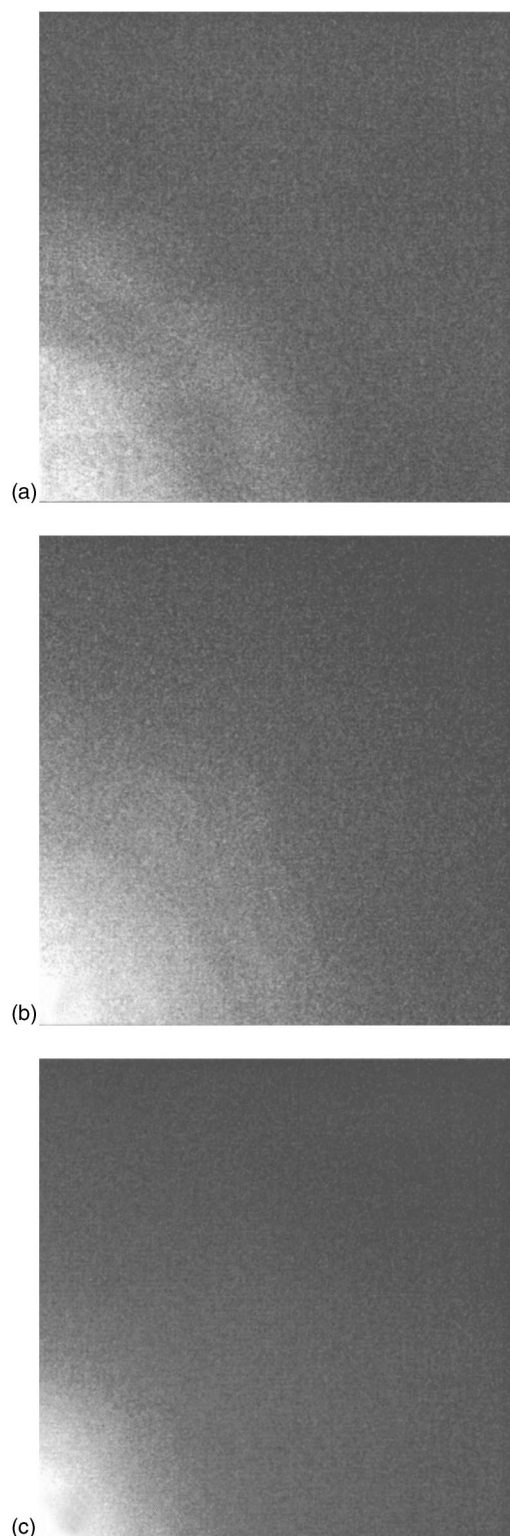


FIG. 2. Nanodiffraction patterns in monocrystalline silicon after: (a) indentation with $P_{\max}=30$ mN, loading/unloading at 0.6 mN/s, (b) indentation with $P_{\max}=30$ mN, loading/unloading at 3 mN/s, and (c) polishing.

sible formation of high-density amorphous structures during indentation loading was proposed.^{11,34} However, no structural information was provided. Based on the fact that the atomic distance of the amorphous structure identified here is close to that of the crystalline β -Sn silicon phase, we believe that on fast loading/unloading, the deformed structure is partly “frozen,” but cannot maintain its crystal configuration and thus relaxes to the amorphous structure which struc-

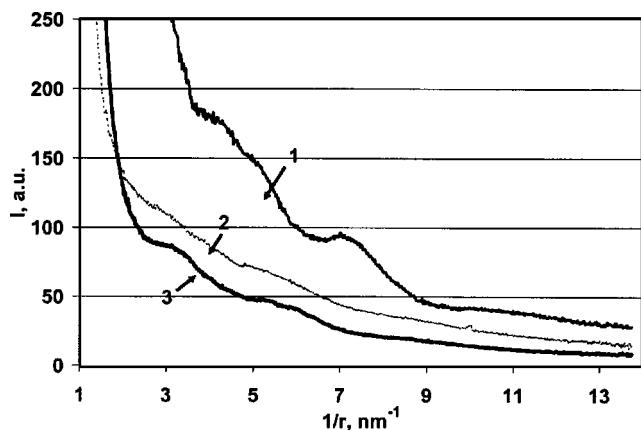


FIG. 3. Scattering intensity of different amorphous structures (obtained by azimuthal averaging, see Ref. 31 for details) in monocrystalline silicon. Curve 1: Indentation with $P_{\max}=30$ mN, loading/unloading at 0.6 mN/s, Curve 2: Polishing; Curve 3: Indentation with $P_{\max}=30$ mN, loading/unloading at 3 mN/s.

turally resembles β -Sn crystalline form with Si coordination of greater than 4.

The situation is different for a slow loading/unloading process [condition (1)]. The corresponding nanodiffraction patterns for the amorphous structures feature a peak at 4.0–4.4 nm⁻¹. It is clear that the peak has shifted to a higher inverse distance when compared with the matching peak for the amorphous structure at fast loading/unloading. The atomic distances were determined to be in the range of 2.26–2.37 Å. These atomic distances are well correlated with the two high-pressure phases,¹⁶ i.e., BC8 phase (having atomic distances of 2.29 Å and 2.37 Å) and R8 phase (having atomic distances of 2.38 Å and 2.39 Å), which were found in the central part of the transformation zone [see Fig. 1(a)]. Again, to understand the formation of the amorphous material, we propose the following scenario for the structural transformation during the indentation: The first structural transformation to β -Sn silicon on loading and the second to R8/BC8 on unloading.^{4,35} The transformation from β -Sn to R8/BC8 needs a minimum time span³⁶ and the peripheral parts of the deformation zone experienced a shorter unloading time so that R8/BC8 phases cannot be completely achieved. Instead, an amorphous structure whose atomic distances close to the R8/BC8 crystalline phases are formed.

The amorphous structure corresponding to polishing [Figs. 1(c) and 2(c), and curve 2 in Fig. 3] features no major peaks as indicated by the corresponding diffraction pattern. This is probably because polishing involves random nanoindentation events³⁷ whose loading and unloading rates are quite varied. In this case, no specific atomic distances or coordination arrangements were developed, and accordingly, no diffused peaks appear within the diffraction pattern.

This study has clearly shown that multiple amorphous structures can be formed by varying loading/unloading conditions during an indentation process. This is in contrast with single tetragonal amorphous structure produced by the diamond anvil cell experiment.¹ This is caused by the difference in stress fields. In a diamond anvil cell experiment,³⁶ shear stresses and residual stresses are minor if they exist, but in indentation the magnitude of stresses is significant.

In conclusion, different amorphous structures have been induced in indentation and polishing in monocrystalline silicon. Specifically, it has been found that:

- (1) Amorphous structures formed at low and fast loading/unloading rates are dissimilar and inherit the nearest-neighbor distance of the crystal in which they are developed.
- (2) When the surface is polished, no preferred nearest-neighbor distances or coordination numbers are developed as a result of the random distribution of unloading rates in the process.

The Australian Research Council is acknowledged for their financial support.

- ¹S. K. Deb, M. Wilding, M. Somayazulu, and P. F. McMillan, *Nature* (London) **414**, 528 (2001).
- ²A. Blanco, E. Chomski, S. Grabtchak, M. Ibisate, S. John, and S. W. Leonard, *Nature* (London) **405**, 437 (2000).
- ³N. Yasunaga, in *Advances in Abrasive Technology*, edited by L. C. Zhang and N. Yasunaga (World Scientific, Singapore, 1997), p. 18.
- ⁴I. Zarudi, J. Zou, and L. C. Zhang, *Appl. Phys. Lett.* **82**, 1027 (2003).
- ⁵J. E. Bradby, J. S. Williams, M. V. Wong-Leung, M. V. Swain, and P. Munroe, *Appl. Phys. Lett.* **77**, 3749 (2000).
- ⁶J. E. Bradby, J. S. Williams, M. V. Wong-Leung, M. V. Swain, and P. Munroe, *J. Mater. Res.* **16**, 1500 (2001).
- ⁷D. L. Callagan and J. C. Morris, *J. Mater. Res.* **7**, 1614 (1992).
- ⁸W. C. D. Cheong and L. C. Zhang, *Nanotechnology* **11**, 173 (2000).
- ⁹J. Crain, G. J. Ackland, J. R. Maclean, R. O. Piltz, P. D. Hatton, and G. S. Pawley, *Phys. Rev. B* **50**, 13043 (1994).
- ¹⁰V. Domnich, Y. G. Gogotsi, and M. Trenary, *Mater. Res. Soc. Symp. Proc.* **649**, Q8.9.1 (2001).
- ¹¹D. Ge, V. Domnich, and Y. Gogotsi, *J. Appl. Phys.* **93**, 2418 (2003).
- ¹²J. Z. Hu, L. D. Merkle, C. S. Menoni, and I. L. Spain, *Phys. Rev. B* **34**, 4679 (1986).
- ¹³A. Keiler, Y. G. Gogotsi, and K. G. Nickel, *J. Appl. Phys.* **81**, 3057 (1997).
- ¹⁴A. B. Mann, D. v. Heerden, J. B. Pethica, and T. P. Weihs, *J. Mater. Res.* **15**, 1754 (2000).
- ¹⁵A. Mann, D. van Heerden, J. Pethica, P. Bowes, and T. Weihs, *Philos. Mag. A* **82**, 1921 (2002).
- ¹⁶R. O. Piltz, S. J. Macleans, S. J. Clark, G. L. Ackland, P. D. Hatton, and J. Crain, *Phys. Rev. B* **52**, 4072 (1995).
- ¹⁷A. Mujica, S. Radescu, A. Munoz, and R. J. Needs, *Phys. Status Solidi B* **223**, 379 (2001).
- ¹⁸I. Zarudi, L. C. Zhang, and M. V. Swain, *Appl. Phys. Lett.* **82**, 1027 (2003).
- ¹⁹J. Fortner and J. S. Lannin, *Phys. Rev. B* **39**, 5527 (1989).
- ²⁰S. Kugler, *Phys. Rev. B* **48**, 7685 (1993).
- ²¹S. C. Moss and J. F. Graczyk, *Phys. Rev. B* **23**, 1167 (1969).
- ²²K. Laaziri, S. Kucia, S. Roorda, M. Chicoine, J. L. Robertson, J. Wang, and S. C. Moss, *Phys. Rev. Lett.* **82**, 3460 (1999).
- ²³D. L. Williamson, S. Roorda, M. Chicoine, R. Tabti, P. A. Stolk, S. Acco, and F. W. Saris, *Appl. Phys. Lett.* **67**, 226 (1995).
- ²⁴D. R. Clarke, M. C. Kroll, P. D. Kirchner, and R. F. Cook, *Phys. Rev. Lett.* **60**, 2156 (1988).
- ²⁵A. Kailer, Y. G. Gogotsi, and K. G. Nickel, *J. Appl. Phys.* **81**, 3057 (1997).
- ²⁶H. Schober, M. Koza, A. Tolle, F. Fujara, C. A. Angell, and R. Bohmer, *Physica B* **241–243**, 897 (1998).
- ²⁷P. H. Poole, T. Tgande, C. A. Angell, and P. F. McMillan, *Science* **275**, 322 (1997).
- ²⁸M. Durandurdu and D. A. Drabol, *Phys. Rev. B* **67**, 212101 (2003).
- ²⁹I. Zarudi and L. C. Zhang, *Tribol. Int.* **32**, 701 (1999).
- ³⁰W. McBride and D. J. H. Cockayne, *J. Non-Cryst. Solids* **318**, 233 (2003).
- ³¹W. McBride, D. J. H. Cockayne, and K. Tsuda, *Ultramicroscopy* **94**, 305 (2004).
- ³²W. H. Press, S. A. Teukolsky, W. T. Vetterling, and B. P. Flannery, *Numerical Recipes in Fortran: The Art of Scientific Computing*, 2nd ed. (Cambridge University Press, Cambridge, 1992).
- ³³J. Donohue, *The Structure of the Elements* (Wiley, New York, 1974).
- ³⁴Y. Q. Wu, X. Y. Yang, and Y. B. Xu, *Acta Mater.* **47**, 2431 (1999).
- ³⁵I. Zarudi, L. C. Zhang, J. Zou, and T. Vodenitcharova, *J. Mater. Res.* **19**, 332 (2004).
- ³⁶I. Zarudi, L. C. Zhang, and M. V. Swain, *J. Mater. Res.* **18**, 758 (2003).
- ³⁷L. C. Zhang and I. Zarudi, *Wear* **225**, 669 (1999).